

# Level anti-crossing spectra of nitrogen-vacancy centers in diamond detected by using modulation of the external magnetic field

S. V. Anishchik<sup>1,\*</sup> and K. L. Ivanov<sup>2,3</sup>

<sup>1</sup>*Voevodsky Institute of Chemical Kinetics and Combustion SB RAS, 630090, Novosibirsk, Russia*

<sup>2</sup>*International Tomography Center SB RAS, 630090, Novosibirsk, Russia*

<sup>3</sup>*Novosibirsk State University, 630090, Novosibirsk, Russia*

We report a study of the magnetic field dependence of the photo-luminescence of  $NV^-$  centers (negatively charged nitrogen-vacancy centers) in diamond single crystals. In such a magnetic field dependence characteristic lines are observed, which are coming from Level Anti-Crossings (LACs) in the coupled electron-nuclear spin system. For enhancing the sensitivity, we used lock-in detection to measure the photo-luminescence intensity and observed a remarkably strong dependence of the LAC-derived lines on the modulation frequency. Upon decreasing of the modulation frequency from 12 kHz to 17 Hz the amplitude of the lines increases by approximately two orders of magnitude. To take a quantitative account for such effects, we developed a theoretical model, which describes the spin dynamics in the coupled electron-nuclear spin system under the action of an oscillating external magnetic field. Good agreement between experiments and theory allows us to conclude that the observed effects are originating from coherent spin polarization exchange in the  $NV^-$  center. Our results are of great practical importance allowing one to optimize the experimental conditions for probing LAC-derived lines in diamond defect centers.

PACS numbers: 61.72.jn, 75.30.Hx, 78.55.-m, 81.05.ug

## I. INTRODUCTION

The negatively charged nitrogen-vacancy center ( $NV^-$  center) in diamond is of great interest due to its unique properties<sup>1</sup>.  $NV^-$  centers are promising systems for numerous applications, in particular, for quantum information processing<sup>2-15</sup> and nanoscale magnetometry<sup>16-21</sup>. It is well-known that under optical excitation the triplet ground state of an  $NV^-$  center acquires strong electron spin polarization. Due to magnetic dipole-dipole interactions between  $NV^-$  centers and other paramagnetic defects in the crystal spin polarization exchange can occur. Such a polarization transfer is of relevance for many applications<sup>11,22-24</sup>. An informative method for studying such polarization transfer processes is given by the Level Anti-Crossing (LAC) spectroscopy. At LACs there is no energy barrier for polarization exchange; consequently, coupled spins can exchange polarization. Us usual, by an LAC we mean the following situation: at a particular field strength a pair of levels, corresponding to quantum states  $|K\rangle$  and  $|L\rangle$ , tends to cross but a perturbation  $V_{KL} \neq 0$  lifts the degeneracy of the levels so that the crossing is avoided. It is well-known that at an LAC efficient coherent exchange of populations of the  $|K\rangle$  and  $|L\rangle$  states occurs<sup>25-28</sup>.

LACs give rise to sharp lines in the magnetic field dependence of the photo-luminescence intensity of precisely oriented  $NV^-$  centers. The most prominent line<sup>29</sup> is observed at 1024 G, which comes from an LAC of the triplet levels in the  $NV^-$  center. Other lines are termed, perhaps, misleadingly, cross-relaxation lines<sup>30</sup>. In reality, all these lines are due to the coherent spin dynamics and are caused by spin polarization exchange at LACs of the entire spin system of the interacting defect centers. Thus, it is reasonable to term the observed magnetic field de-

pendences "LAC spectra".

In this work, we report a study of LAC-lines in diamond single crystals by using modulation of the external magnetic field. Generally, such lines are observed by monitoring photo-luminescence as a function of the external magnetic field; a prerequisite for such experiments<sup>29-36</sup> is precise orientation of the diamond crystal (so that the magnetic field is parallel to [111] crystal axis with a precision of better than one tenth of a degree). Typically, the LAC-line at 1024 G is relatively easy to detect; however, observing weaker satellite lines and lines coming from interaction with other paramagnetic centers is technically more demanding. In a previous work<sup>36</sup> this problem was minimized by using a lock-in detection: such a method provides much better sensitivity to weaker lines. In experiments using lock-in detection the external field strength is modulated at a frequency  $f_m$ ; the output luminescence signal is multiplied by the reference signal given by  $\sin(2\pi f_m t)$  (or  $\cos(2\pi f_m t)$ ) and integrated to provide an increased sensitivity to weak signals. In experiments using lock-in detection<sup>36</sup> a new LAC line at zero magnetic field has been detected; groups of LAC-lines around 490-540 G, 590 G and 1024 G are clearly seen. The shape of the lines ("dispersive" lineshape) is different from that in conventional field-swept experiments: each line has a positive and a negative component; at the center of each line the signal intensity is zero. At first glance, such an appearance of the LAC-lines ("derivative" spectrum) is standard for experiments using lock-in detection. However, here we demonstrate an unexpected behavior of the LAC-lines, namely, a substantial increase of the line intensity upon decrease of the modulation frequency.

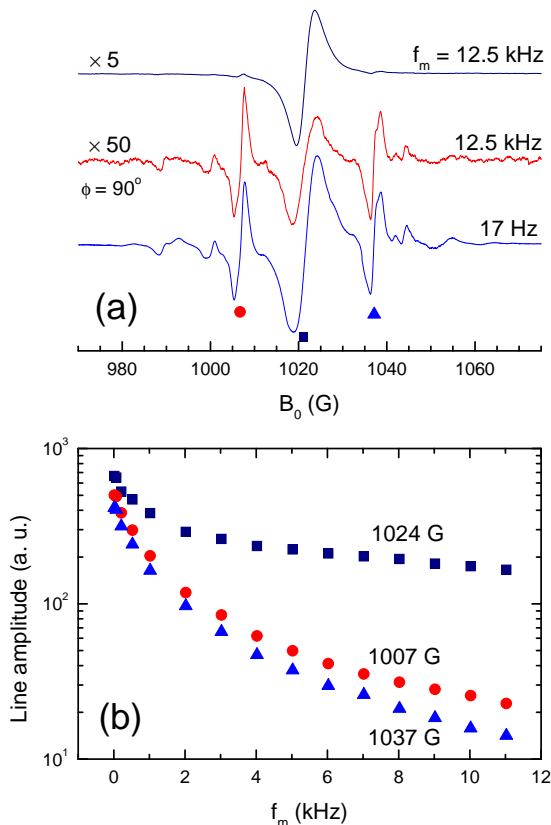


FIG. 1. (a) Experimental LAC spectra of  $\text{NV}^-$  centers in a diamond single crystal in the magnetic field range 970-1075 G. For each curve we give the  $f_m$  value used in experiments. For the upper curve the phase of the lock-in detector is chosen such that the signal for the central LAC-line is maximal. For the middle trace the phase is shifted by  $90^\circ$  with respect to that for the upper curve. The amplitude of the upper curve is increased by a factor of 5, for the middle curve – by a factor of 50. The LAC-lines are indicated by circle, square and triangle. (b) Dependence of the amplitude of the three LAC-lines (symbols correspond to LAC-lines in subplot a) on the modulation frequency  $f_m$ . For each curve the magnetic field strength  $B_0$  corresponding to the center of the corresponding line is specified. For each experimental point the lock-in detector phase is set such that the amplitude of the corresponding line was maximal. In all cases the modulation amplitude was  $B_m = 0.5$  G.

## II. METHODS

The experimental method is described in detail in a previous publication<sup>36</sup>.

Experiments were carried out using single crystals of a synthetic diamond grown at high temperature and high pressure in a Fe-Ni-C system. As-grown crystals were irradiated by fast electrons of an energy of 3 MeV; the irradiation dose was  $10^{18}$  el/cm<sup>2</sup>. After that the samples were annealed during two hours in vacuum at a temperature of  $800^\circ$ . The average concentration of  $\text{NV}^-$  centers was  $9.3 \times 10^{17}$  cm<sup>-3</sup>.

The samples were placed in a magnetic field, which is

a superposition of the permanent field,  $B_0$ , and a weak field modulated at the frequency  $f_m$ :

$$B = B_0 + B_m \sin(2\pi f_m t), \quad (1)$$

and irradiated by the laser light at a wavelength of 532 nm (irradiation power was 400 mW). The beam direction was parallel to the magnetic field vector  $\mathbf{B}_0$ . The laser light was linearly polarized and the electric field vector  $\mathbf{E}$  was perpendicular to  $\mathbf{B}_0$ . The luminescence intensity was measured by a photo-multiplier. The resulting signal was sent to the input of the lock-in detector. The modulation frequency  $f_m$  was varied from 10 Hz to 100 kHz.

## III. RESULTS AND DISCUSSION

Experimental results are presented in Fig. 1. Fig. 1(a) shows the LAC-spectra of the  $\text{NV}^-$  center in the field range around 1024 G where the well-known LAC-line is located. The spectra shown for two different modulation frequencies, 12.5 kHz and 17 Hz, are remarkably different. As it is seen from the Figure, when  $f_m = 12.5$  kHz and the lock-in detector phase set such that the central line at 1024 G has the maximal intensity, the satellite lines at 1007 G and 1037 G are hardly visible. These lines are originating from polarization exchange between the spin-polarized  $\text{NV}^-$  center and neutral nitrogen atoms (spin-1/2 defect centers), replacing carbons in the diamond lattice<sup>35</sup>. Polarization transfer occurs when the level splittings in both defect centers become equal to each other (causing a level crossing): under such conditions dipole-dipole interaction turns a level crossing into an LAC and enables coherent polarization exchange. Such a polarization transfer is usually termed (perhaps, erroneously) cross-relaxation<sup>30</sup>. The weak amplitude of the satellite lines is due to the weak interaction between different defect centers. Consequently, the time response of the system (in other words, the characteristic time of the polarization transfer) is much longer than the period of modulation,  $T = 1/f_m$ . Therefore, there is a phase shift of about  $90^\circ$ : using such a phase shift we clearly observe the satellite lines. Interestingly, many weak additional lines are seen when a phase shift is introduced.

When the modulation frequency is reduced to 17 Hz the amplitude of the central line increases by a factor of 7, whereas the satellite lines become 50 times more intense. At such a low frequency the phase shift for all lines is very small. As it is seen from the LAC-spectrum there are no new lines appearing in the spectrum but the signal-to-noise ratio is substantially increased.

In Fig. 1(b) we present the experimental dependences of the line intensity, as determined for the three different LAC-lines, on the modulation frequency. Here the total peak-to-peak amplitude is presented; the lock-in detector phase was set such that for each experiment the amplitude of the corresponding line was maximal.

It is clearly seen that by varying the modulation frequency we obtained a strong variation of the LAC-line intensities by roughly two orders of magnitude. Interestingly, in the assessed frequency range the dependence is non-exponential; the slope of the curve increases at lower modulation frequencies.

The most unexpected effect is that the increase of the line intensity is occurring at modulation frequencies, which are much smaller than the relaxation rates of the  $NV^-$  center (when measured in the same units). To rationalize this effect we made attempts to simulate the spin dynamics of a two-level system having an LAC. However, such a model predicts a much smaller effect of  $f_m$ ; moreover, the frequency range where the line intensity strongly varies is completely different from that found experimentally.

The observed strong dependence can be explained by polarization transfer from the electronic triplet spin system to nuclear spins, since the relaxation times of nuclear spins are much longer (by several orders of magnitude) than the electronic spin relaxation times.

To model electron-nuclear polarization transfer we made the following simplifications. First, we did not treat the entire three-level electron spin system but restricted ourselves to only two levels. In such a situation the electronic spin subsystem can be modeled by a fictitious spin  $S = 1/2$ . We also assume that the luminescence intensity is proportional to the population of the  $S_z = 1/2$  state. This is a reasonable assumption because only one of the three triplet states of the  $NV^-$  center gives intense luminescence. Hereafter we assume that the  $z$ -axis is parallel to the external magnetic field. The  $S$  spin interacts with the permanent external  $B_0$  field, with the oscillating  $B_m$  field and with surrounding nuclear spins by hyperfine coupling (HFC), which is assumed to be isotropic. For the sake of simplicity, we reduced the nuclear spin subsystem to only one spin  $I = 1/2$ . Then the Hamiltonian of the spin system under consideration takes the form (in  $\hbar$  units):

$$\hat{H}(t) = \gamma B_0 \hat{S}_z + V \hat{S}_x + A(\hat{\mathbf{S}} \cdot \hat{\mathbf{I}}) + \Omega_1 \cos(2\pi f_m t) \hat{S}_z, \quad (2)$$

where  $\hat{\mathbf{S}}$  and  $\hat{\mathbf{I}}$  are the spin operators of the electron and the nucleus, respectively,  $\gamma$  is the electronic gyromagnetic ratio,  $B_0$  is the external magnetic field strength,  $V$  is an external perturbation (coming, e.g., from a small misalignment of the crystal),  $A$  is the isotropic HFC constant,  $\Omega_1$  is the amplitude of the modulated magnetic field,  $f_m$  is the modulation frequency. Hereafter we use the notation  $\gamma B_0 = \omega_0$ . Considering only the main part of the Hamiltonian,  $H_0 = \gamma B_0 \hat{S}_z$  we obtain that there is a level crossing at  $B_0 = 0$ ; however, the perturbations given by  $V$  and  $A$  mix the crossing levels and turn this crossing into an LAC. By turning on the modulation we introduce repeated passages through the LAC; upon these passages spin evolution is taking place resulting in redistribution of polarization.

Qualitatively, we expect different regimes for spin dynamics at low and at high  $f_m$ . At a low  $f_m$  each passage through the LAC results in adiabatic inversion of populations of the  $S$ -spin states. Consequently, the luminescence signal is expected to be modulated at the  $f_m$  frequency having the maximal possible amplitude and the same phase as the modulated external field. During a fast passage through the LAC, i.e., at large  $f_m$ , the populations are mixed only slightly and the amplitude of modulation of the luminescence signal is expected to drop down. In addition, the modulation of the signal is no longer in-phase with the reference signal of the lock-in amplifier, resulting in strong phase shifts of the signal. As we show below, the calculation results are in good agreement with these expectations.

The spin evolution is described by the Liouville-von Neumann equation:

$$\frac{d\rho_{ij}}{dt} = L_{ij;kl}(t)\rho_{kl}, \quad (3)$$

where  $\rho$  is the density matrix of the two-spin electron-nuclear system in the Liouville representation (column-vector with 16 elements), while the elements of the  $\hat{\hat{L}}$  super-operator are as follows:

$$L_{ij;kl} = i(\delta_{ik}H_{lj} - \delta_{jl}H_{ik}) + R_{ij;kl}, \quad (4)$$

where  $R_{ij;kl}$  is the relaxation matrix. To specify the  $R$  super-operator we made the following simplifying assumptions. We treated two contributions to the electron spin relaxation, the spin-lattice relaxation (at a rate  $R_1$ ) and phase relaxation (at a rate  $R_2$ ). In addition, we take into account photo-excitation of the  $NV^-$  center, which produces the electron spin polarization, i.e., the population difference for the states of the  $S$ -spin. This process is considered in a simplified manner as transitions from the  $S_z = -1/2$  state ( $\alpha$ -state) to the  $S_z = +1/2$  state ( $\beta$ -state) at a rate  $I$  (pumping rate for the electron spin polarization). Relaxation of the nuclear spin is completely neglected because it is usually much slower than that for the electron spin.

The period  $T = 1/f_m$  was split into  $N$  equal intervals of a duration  $\Delta t = T/N$ . In each step, the density matrix  $\rho$  was propagated by using a matrix exponent:

$$\rho(t + \Delta t) = \exp[\hat{\hat{L}}(t)\Delta t]\rho(t). \quad (5)$$

Generally, the solution depends on the initial conditions. However, in the present case we are interested in the "steady-state" solution, which is reached after many modulation periods. Indeed, in experiments transient effects are not important because signal averaging is performed over many  $T$  periods (only the steady-state of the system is probed). To obtain such a solution of eq. (3) we assume that the density matrix before a period of modulation,  $\rho(0)$ , is the same as that after the period:

$$\begin{aligned} \rho(0) = \rho(T) = & \exp[\hat{\hat{L}}(t = T - \Delta t)\Delta t] \times \dots \\ & \times \exp[\hat{\hat{L}}(t = 0)\Delta t]\rho(0) = \hat{\hat{U}}\rho(0). \end{aligned} \quad (6)$$

Here  $\hat{U}$  is the super-matrix, which describes the evolution over a single modulation period. This equation is a linear equation for the  $\rho(0)$  vector. To find a non-trivial solution of such a matrix equation, we need to exclude one equation from the system (the one, which linearly depends on other equations) and to replace it by the following one:  $\sum_i \rho_{ii}(0) = 1$ , which describes nothing else but conservation of the trace of the density matrix. This new system can be solved by using standard linear algebra methods. The  $\hat{U}$  matrix was computed numerically; to do so we set the value of  $N$  such that further increase of  $N$  changed the final results by less than 1%. Of course, it is necessary to increase  $N$  substantially at small  $f_m$ . At the lowest modulation frequency we used  $N = 4 \times 10^5$ .

To compare theoretical results to the experimental data we numerically computed the sine and cosine Fourier components of the element of interest of the density matrix, namely, the population of the  $\alpha$ -state,  $\rho_{\alpha\alpha}$ . This element can be computed when  $\rho(t)$  is known:

$$X = \frac{1}{T} \int_0^T \rho_{\alpha\alpha} \cos(2\pi f_m t) dt, \quad (7)$$

$$Y = \frac{1}{T} \int_0^T \rho_{\alpha\alpha} \sin(2\pi f_m t) dt. \quad (8)$$

So, essentially, we calculate polarization of the  $S$ -spin, which is given by the difference  $[\rho_{\alpha\alpha} - 1/2]$ . In the same way we can compute polarization of the  $I$ -spin. Knowing  $X$  and  $Y$  we can completely characterize the signal. An analogue of the lock-in detector phase variation by an angle  $\phi$  is the rotation of axes in the functional space:

$$X' = X \cos \phi + Y \sin \phi. \quad (9)$$

In Fig. 2 we present the magnetic field dependences of the Fourier  $X$  and  $Y$  components of the electron and nuclear polarization. Additionally, for the electron spin the  $X'$  component is presented at specific values of the lock-in detector phase  $\phi$ . The  $\phi$  phase was set such that the line intensity was maximal. One can readily see that at the lowest modulation frequency the LAC-spectra for the electron and nuclear spins are the same, resembling a dispersive Lorentzian line. At higher  $f_m$  frequencies the line shape is significantly distorted and line intensity decreases. Interestingly, polarization of the nuclear spin drops faster than that for the electron spin.

In Fig. 3 we present the calculated LAC-line intensity as functions of the modulation frequency  $f_m$ ; the dependences are calculated upon systematic variation of the relevant parameters. In all cases, upon decrease of the modulation frequency by two orders of magnitude, i.e., from 1 to 0.01, the line intensity increases by roughly two orders of magnitude. It also turned out that the external perturbation is of great importance: at  $V \rightarrow 0$  the line intensity also tends to zero. The line intensity

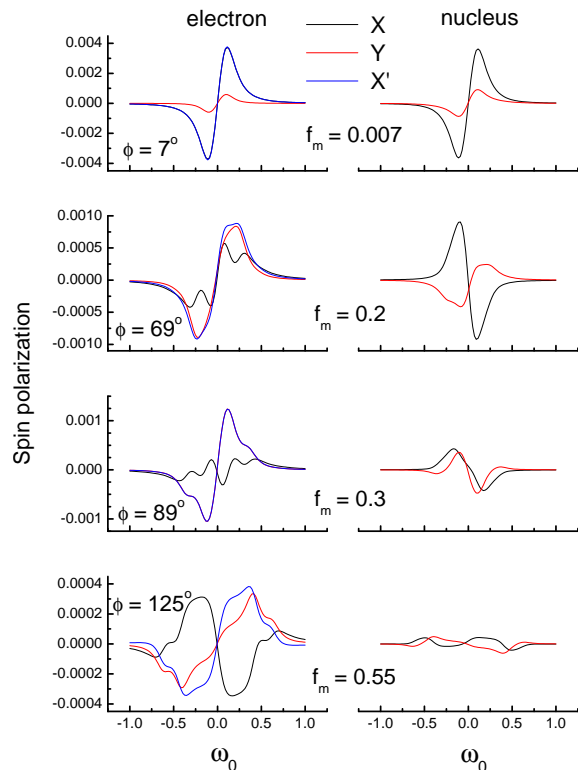


FIG. 2. Theoretical LAC-spectra for different  $f_m$  frequencies. Calculation parameters:  $R_1 = 0.1$ ,  $R_2 = 0.1$ ,  $I = 0.01$ ,  $V = 0.1$ ,  $A = 0.2$ ,  $\Omega_1 = 0.1$ . The  $f_m$  value is given for each curve. The values of all parameter are given in arbitrary frequency units.

also drops down upon decrease of the  $I$  parameter, simply because of the lower efficiency of polarization formation. Likewise, the LAC-line intensity is reduced upon decrease of the modulation amplitude,  $\Omega_1$ ; interestingly, there is no simple proportionality relation between the line intensity and  $\Omega_1$ . The dependence on the HFC constant,  $A$ , is relatively complicated. Notably, there is a non-monotonous dependence of the LAC-line intensity on the modulation frequency. A plausible explanation of this effect can be deduced from the spectra shown in Fig. 2. It is clearly seen that the width for different Fourier components is considerably different: at high frequencies the sine-component prevails, which is phase-shifted by  $90^\circ$  with respect to the modulation fields, whereas at low frequencies the cosine-component is dominating. At intermediate frequencies both components are of a comparable intensity. As a consequence, the phase shift (required to obtain the highest LAC-line intensity) leads to a distorted LAC-line with two components partly compensating each other. As a result, the total line intensity decreases.

Interestingly, the calculation predicts an even stronger increase of the line intensity at low  $f_m$  frequencies as compared to the experimental data. Furthermore, the theoretical dependence is closer to an exponential behavior (in contrast to the experimental dependence). For fur-

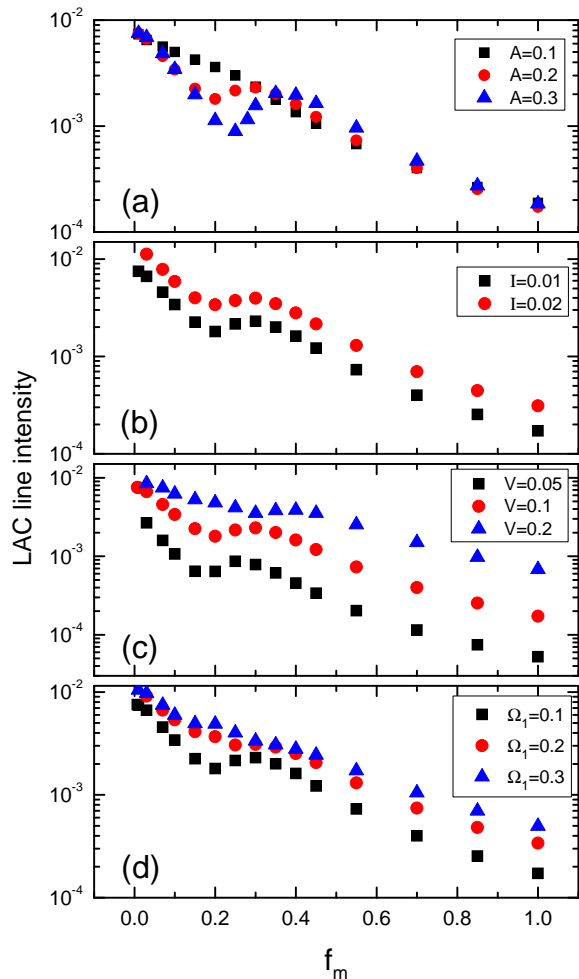


FIG. 3. Calculated dependence of the LAC-line intensity on the modulation frequency  $f_m$ . Here we show the signal components  $X$  and  $Y$ , as well as  $X'$ . Calculation parameters (when different from those given in the figure):  $R_1 = 0.1$ ,  $R_2 = 0.1$ ,  $I = 0.01$ ,  $V = 0.1$ ,  $A = 0.2$ ,  $\Omega_1 = 0.1$ . The values of all parameter are given in arbitrary frequency units.

ther increase of the LAC-line intensity at low frequencies it might be necessary to consider an additional mechanism with even slower response. Such a mechanism<sup>37</sup> could be photo-excitation of the excited state on an  $NV^-$  center to the conduction band, accompanied by the formation of the neutral  $NV^0$  center, which preserves polarization of the nuclear spin. When the backward process (the electron goes to the  $NV^0$  center) takes place, the newly formed  $NV^-$  has no electron spin polarization. However, such polarization can be generated by polarization transfer from the nuclear spin.

#### IV. CONCLUSIONS

We report a study of LAC-lines in  $NV^-$  defect centers in diamond crystals by using lock-in detection of the sig-

nal. Such a method allows one to obtain sharp LAC-lines with excellent signal-to-noise ratio. A strong and unexpected effect of the modulation frequency on the LAC-line intensity is demonstrated. Interestingly, the LAC line is the strongest at low modulation frequencies. Thus, measurements at low  $f_m$  are advantageous, even despite the technical issues concerning experiments at low frequencies (namely, the instrumental noise). Moreover, LAC-spectra obtained at low modulation frequencies are free from distortions and phase shifts of the signal with respect to the reference signal of the lock-in amplifier.

To rationalize the observed effect of the modulation frequency we performed a theoretical study and computed numerically the evolution of the spin system under the action of the modulation field. In the theoretical model, we introduced a single electron spin 1/2 (modeling the electron spin degrees of freedom of the  $NV^-$  center) coupled to a nuclear spin 1/2. Such a model can reproduce the main features found in experiments. Specifically, at low modulation frequency we obtain adiabatic exchange of populations of the states having an LAC. This results in the modulated luminescence signal of the maximal amplitude, which has the same phase as the external magnetic field  $\Omega_1$ . In contrast, at high modulation frequencies spin mixing occurs upon fast passages through the LAC and populations are mixed only slightly. Consequently, the signal drops and becomes distorted. We anticipate that these features can be reproduced also by more elaborate calculations for extended spin systems, which can model, e.g., polarization exchange between different paramagnetic centers in the crystal.

Our work provides useful practical recommendations on how to conduct experimental studies of LAC-lines. As we show in subsequent publications, the experimental method used here indeed enables sensitive detection of LAC-lines and observation of previously unknown LAC-lines. Furthermore, for the first time we demonstrate that modulation (used in lock-in detection) is not only a prerequisite for sensitive detection of weak signals but also a method to affect spin dynamics of  $NV^-$  centers in diamonds.

#### ACKNOWLEDGMENTS

Experimental work was supported by the Russian Foundation for Basic Research (Grant No. 16-03-00672); theoretical work was supported by the Russian Science Foundation (grant No. 15-13-20035).

\* svan@kinetics.nsc.ru

- <sup>1</sup> M. W. Doherty, N. B. Manson, P. Delaney, F. Jelezko, J. Wrachtrup, and L. C. L. Hollenberg, *Physics Reports* **528**, 1 (2013).
- <sup>2</sup> A. Gruber, A. Dräbenstedt, C. Tietz, L. Fleury, J. Wrachtrup, and C. von Borczyskowski, *Science* **276**, 2012 (1997).
- <sup>3</sup> J. Wrachtrup, S. Y. Kilin, and A. P. Nizovtsev, *Optics and Spectroscopy* **91**, 429 (2001).
- <sup>4</sup> F. Jelezko and J. Wrachtrup, *J. Phys.: Condens. Matter* **16**, R1089 (2004).
- <sup>5</sup> L. Childress, M. V. Gurudev Dutt, J. M. Taylor, A. S. Zibrov, F. Jelezko, J. Wrachtrup, P. R. Hemmer, and M. D. Lukin, *Science* **314**, 281 (2006).
- <sup>6</sup> J. Wrachtrup and F. Jelezko, *J. Phys.: Condens. Matter* **18**, S807 (2006).
- <sup>7</sup> R. Hanson, O. Gywat, and D. D. Awschalom, *Phys. Rev. B* **74**, 161203 (2006).
- <sup>8</sup> T. Gaebel, M. Domhan, I. Popa, C. Wittmann, P. Neumann, F. Jelezko, J. R. Rabeau, N. Stavrias, A. D. Greentree, S. Praver, J. Meiler, J. Twamley, P. R. Hemmer, and J. Wrachtrup, *Nat. Phys.* **2**, 408 (2006).
- <sup>9</sup> C. Santori, D. Fattal, S. M. Spillane, M. Fiorentino, R. G. Beausoleil, A. D. Greentree, P. Olivero, M. Draganski, J. R. Rabeau, P. Reichart, B. C. Gibson, S. Rubanov, D. N. Jamieson, and S. Praver, *Opt. Express* **14**, 7986 (2006).
- <sup>10</sup> F. C. Waldermann, P. Olivero, J. Nunn, K. Surmacz, Z. Y. Wang, D. Jaksch, R. A. Taylor, I. A. Walmsley, M. Draganski, P. Reichart, A. D. Greentree, D. N. Jamieson, and S. Praver, *Diamond and Rel. Mat.* **16**, 1887 (2007).
- <sup>11</sup> P. C. Maurer, G. Kucsko, C. Latta, L. Jiang, N. Y. Yao, S. D. Bennett, F. Pastawski, D. Hunger, N. Chisholm, M. Markham, D. J. Twitchen, J. I. Cirac, and M. D. Lukin, *Science* **336**, 1283 (2012).
- <sup>12</sup> T. van der Sar, Z. H. Wang, M. S. Blok, H. Bernien, T. H. Taminiiau, D. M. Toyli, D. A. Lidar, D. D. Awschalom, R. Hanson, and V. V. Dobrovitski, *Nature (London)* **484**, 82 (2012).
- <sup>13</sup> F. Dolde, I. Jakobi, B. Naydenov, N. Zhao, S. Pezzagna, C. Trautmann, J. Meijer, P. Neumann, F. Jelezko, and J. Wrachtrup, *Nature Physics* **9**, 139 (2013).
- <sup>14</sup> F. Dolde, V. Bergholm, Y. Wang, I. Jakobi, B. Naydenov, S. Pezzagna, J. Meijer, F. Jelezko, P. Neumann, T. Schulte-Herbrüggen, B. Jacob, and J. Wrachtrup, *Nature Communications* **5**, 3371 (2014).
- <sup>15</sup> W. Pfaff, B. Hensen, H. Bernien, S. B. van Dam, M. S. Blok, T. H. Taminiiau, M. J. Tiggelman, R. N. Schouten, M. Markham, D. J. Twitchen, and R. Hanson, *Science* **345**, 532 (2014).
- <sup>16</sup> J. M. Taylor, P. Cappellaro, L. Childress, L. Jiang, D. Budker, P. R. Hemmer, A. Yacoby, R. Walsworth, and M. D. Lukin, *Nature Physics* **4**, 810 (2008).
- <sup>17</sup> G. Balasubramanian, I. Y. Chan, R. Kolesov, M. Al-Hmoud, J. Tisler, C. Shin, C. Kim, A. Wojcik, P. R. Hemmer, A. Krueger, T. Hanke, A. Leitenstorfer, R. Bratschitsch, F. Jelezko, and J. Wrachtrup, *Nature (London)* **455**, 648 (2008).
- <sup>18</sup> J. R. Maze, P. L. Stanwix, J. S. Hodges, S. Hong, J. M. Taylor, P. Cappellaro, L. Jiang, M. V. Gurudev Dutt, E. Togan, A. S. Zibrov, A. Yacoby, R. L. Walsworth, and M. D. Lukin, *Nature (London)* **455**, 644 (2008).
- <sup>19</sup> E. Rittweger, K. Y. Han, S. E. Irvine, C. Eggeling, and S. W. Hell, *Nature Photonics* **3**, 144 (2009).
- <sup>20</sup> V. M. Acosta, E. Bauch, M. P. Ledbetter, C. Santori, K.-M. C. Fu, P. E. Barclay, R. G. Beausoleil, H. Linget, J. F. Roch, F. Treussart, S. Chemerisov, W. Gawlik, and D. Budker, *Phys. Rev. B* **80**, 115202 (2009).
- <sup>21</sup> K. Fang, V. M. Acosta, C. Santori, Z. Huang, K. M. Itoh, H. Watanabe, S. Shikata, and R. G. Beausoleil, *Phys. Rev. Lett.* **110**, 130802 (2013).
- <sup>22</sup> A. Jarmola, A. Berzins, J. Smits, K. Smits, J. Prikulis, F. Gahbauer, R. Ferber, D. Erts, M. Auzinsh, and D. Budker, *Appl. Phys. Lett.* **107**, 242403 (2015).
- <sup>23</sup> M. Mrózek, D. Rudnicki, P. Kehayias, A. Jarmola, D. Budker, and W. Gawlik, *EPJ Quantum Technol.* (2015), doi:10.1140/epjqt/s40507-015-0035-z.
- <sup>24</sup> Q. Chen, I. Schwarz, F. Jelezko, A. Retzker, and M. B. Plenio, *Phys. Rev. B* **93**, 060408 (2016).
- <sup>25</sup> F. D. Colegrove, P. A. Franken, R. R. Lewis, and R. H. Sands, *Phys. Rev. Lett.* **3**, 420 (1959).
- <sup>26</sup> K. L. Ivanov, A. N. Pravdivtsev, A. V. Yurkovskaya, H.-M. Viethd, and R. Kaptein, *Prog. NMR Spectrosc.* **81**, 1 (2014).
- <sup>27</sup> A. N. Pravdivtsev, A. V. Yurkovskaya, N. N. Lukzen, H.-M. Viethd, and K. L. Ivanov, *Phys. Chem. Chem. Phys.* **16**, 18707 (2014).
- <sup>28</sup> H. Clevenson, E. H. Chen, F. Dolde, C. Teale, D. Englund, and B. D., *Phys. Rev. A* **94**, 021401 (2016).
- <sup>29</sup> R. J. Epstein, F. M. Mendoza, Y. K. Kato, and D. D. Awschalom, *Nat. Phys.* **1**, 94 (2005).
- <sup>30</sup> E. van Oort and M. Glasbeek, *Phys. Rev. B* **40**, 6509 (1989).
- <sup>31</sup> R. Hanson, F. Mendoza, R. Epstein, and D. Awschalom, *Phys. Rev. Lett.* **97**, 087601 (2006).
- <sup>32</sup> L. J. Rogers, S. Armstrong, M. J. Sellars, and N. B. Manson, *New Journal of Physics* **10**, 103024 (2008).
- <sup>33</sup> L. J. Rogers, R. L. McMurtrie, M. J. Sellars, and N. B. Manson, *New Journal of Physics* **11**, 063007 (2009).
- <sup>34</sup> N. Lai, D. Zheng, F. Jelezko, F. Treussart, and J.-F. Roch, *Appl. Phys. Lett.* **95**, 133101 (2009).
- <sup>35</sup> S. Armstrong, L. J. Rogers, R. L. McMurtrie, and N. B. Manson, *Physics Procedia* **3**, 1569 (2010).
- <sup>36</sup> S. V. Anishchik, V. G. Vins, A. P. Yelissev, N. N. Lukzen, N. L. Lavrik, and V. A. Bagryansky, *New J. Phys.* **17**, 023040 (2015).
- <sup>37</sup> P. Siyushev, H. Pinto, M. Vörös, A. Gali, F. Jelezko, and J. Wrachtrup, *Phys. Rev. Lett.* **110**, 167402 (2013).